

Field strength correlators in QCD at zero and non-zero temperature

A. Di Giacomo ^a, E. Meggiolaro ^{a *} and H. Panagopoulos ^b

^aDipartimento di Fisica dell'Università and I.N.F.N., Sezione di Pisa,
I-56100 Pisa, Italy.

^bDepartment of Natural Sciences, University of Cyprus,
1678 Nicosia, Cyprus.

We study, by numerical simulations on a lattice, the behaviour of the gauge-invariant field strength correlators in QCD both at zero temperature, down to a distance of 0.1 fm, and at finite temperature, across the deconfinement phase transition.

1. INTRODUCTION

An important role in hadron physics is played by the gauge-invariant two-point correlators of the field strengths in the QCD vacuum. They are defined as

$$\mathcal{D}_{\mu\rho,\nu\sigma}(x) = \langle 0 | \text{Tr} \{ G_{\mu\rho}(x) S G_{\nu\sigma}(0) S^\dagger \} | 0 \rangle, \quad (1)$$

where $G_{\mu\rho} = g T^a G_{\mu\rho}^a$ is the field-strength tensor and $S = S(x, 0)$ is the Schwinger phase operator needed to parallel-transport the tensor $G_{\nu\sigma}(0)$ to the point x .

These correlators govern the effect of the gluon condensate on the level splittings in the spectrum of heavy $Q\bar{Q}$ bound states [1–3]. They are the basic quantities in models of stochastic confinement of colour [4–6] and in the description of high-energy hadron scattering [7–10].

A numerical determination of the correlators on lattice (with gauge group $SU(3)$) already exists, in the range of physical distances between 0.4 and 1 fm [11]. In that range $\mathcal{D}_{\mu\rho,\nu\sigma}$ falls off exponentially

$$\mathcal{D}_{\mu\rho,\nu\sigma}(x) \sim \exp(-|x|/\lambda), \quad (2)$$

with a correlation length $\lambda \simeq 0.22$ fm [11].

What makes the determination of the correlators possible on the lattice, with a reasonable computing power, is the idea [12,13] of removing the effects of short-range fluctuations on large distance correlators by a local *cooling* procedure.

*Speaker at the conference.

Freezing the links of QCD configurations one after the other, damps very rapidly the modes of short wavelength, but requires a number n of cooling steps proportional to the square of the distance d in lattice units to affect modes of wavelength d :

$$n \simeq k d^2. \quad (3)$$

Cooling is a kind of diffusion process. If d is sufficiently large, there will be a range of values of n in which lattice artefacts due to short-range fluctuations have been removed, without touching the physics at distance d ; by *lattice artefacts* we mean statistical fluctuations and renormalization effects from lattice to continuum. This removal will show up as a plateau in the dependence of the correlators on n . This was the technique successfully used in Ref. [11]. There, the range of distances explored was from 3–4 up to 7–8 lattice spacings at $\beta \simeq 6$ ($\beta = 6/g^2$), which means approximately from 0.4 up to 1 fm in physical distance. The lattice size was 16^4 .

In Sect. 2 we discuss new results obtained on a 32^4 lattice, at β between 6.6 and 7.2: at these values of β the lattice size is still bigger than 1 fm, and therefore safe from infrared artefacts, but $d = 3, 4$ lattice spacings now correspond to physical distances of about 0.1 fm. Since what matters to our cooling procedure is the distance in lattice units, we obtain in this way a determination of the correlators at distances down to 0.1 fm [14].

All of the above concerns the theory at zero temperature. In Sect. 3 we go further and de-

termine the behaviour of the correlators at finite temperature for the pure-gauge theory with $SU(3)$ colour group and in particular we study their behaviour across the deconfining phase transition [15]. The motivations to do that stem from Refs. [16–18].

2. RESULTS AT $T = 0$

The most general form of the correlator compatible with the invariances of the system at zero temperature is [4–6]

$$\begin{aligned} \mathcal{D}_{\mu\rho,\nu\sigma}(x) = & (\delta_{\mu\nu}\delta_{\rho\sigma} - \delta_{\mu\sigma}\delta_{\rho\nu}) [\mathcal{D}(x^2) + \mathcal{D}_1(x^2)] \\ & + (x_\mu x_\nu \delta_{\rho\sigma} - x_\mu x_\sigma \delta_{\rho\nu} + x_\rho x_\sigma \delta_{\mu\nu} \\ & - x_\rho x_\nu \delta_{\mu\sigma}) \frac{\partial \mathcal{D}_1(x^2)}{\partial x^2}. \end{aligned} \quad (4)$$

\mathcal{D} and \mathcal{D}_1 are invariant functions of x^2 . We work in the Euclidean region.

It is convenient to define a $\mathcal{D}_\parallel(x^2)$ and a $\mathcal{D}_\perp(x^2)$ as follows:

$$\begin{aligned} \mathcal{D}_\parallel &\equiv \mathcal{D} + \mathcal{D}_1 + x^2 \frac{\partial \mathcal{D}_1}{\partial x^2}, \\ \mathcal{D}_\perp &\equiv \mathcal{D} + \mathcal{D}_1. \end{aligned} \quad (5)$$

On the lattice we can define a lattice operator $\mathcal{D}_{\mu\rho,\nu\sigma}^L$, which is proportional to $\mathcal{D}_{\mu\rho,\nu\sigma}$ in the naïve continuum limit, i.e., when the lattice spacing $a \rightarrow 0$. Making use of the definition (5) we can thus write, in the same limit,

$$\begin{aligned} \mathcal{D}_\parallel^L(\hat{d}a) &\underset{a \rightarrow 0}{\sim} a^4 \mathcal{D}_\parallel(d^2 a^2) + \mathcal{O}(a^6), \\ \mathcal{D}_\perp^L(\hat{d}a) &\underset{a \rightarrow 0}{\sim} a^4 \mathcal{D}_\perp(d^2 a^2) + \mathcal{O}(a^6). \end{aligned} \quad (6)$$

Equations (6) come from a formal expansion of the operator, and are expected to be modified, when the expectation value is computed, by lattice artefacts, i.e., by effects due to the ultraviolet *cutoff*. These effects can be estimated in perturbation theory and subtracted [19]. Instead we remove them by cooling the quantum fluctuations at the scale of the lattice spacing, as explained in the Introduction. After cooling, \mathcal{D}_\parallel^L and \mathcal{D}_\perp^L are expected to obey Eqs. (6). The typical behaviour of \mathcal{D}_\parallel^L and of \mathcal{D}_\perp^L along cooling is shown in Fig. 1. Our data are the values of the correlations at the plateau.

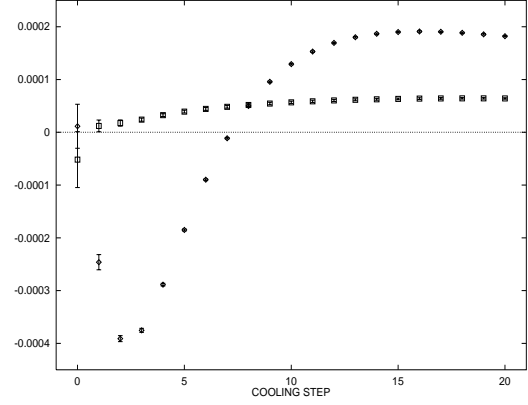


Figure 1. A typical behaviour of \mathcal{D}_\parallel^L (diamonds; $d = 6$, $\beta = 6.6$, lattice 32^4) and of \mathcal{D}_\perp^L (squares; $d = 12$, $\beta = 6.6$, lattice 32^4) during cooling.

We have measured the correlations on a 32^4 lattice at distances ranging from 3 to 14 lattice spacings and at $\beta = 6.6, 6.8, 7.0, 7.2$. From renormalization group arguments,

$$a(\beta) = \frac{1}{\Lambda_L} f(\beta), \quad (7)$$

where Λ_L is the fundamental mass-scale of QCD in the lattice renormalization scheme. At large enough β , $f(\beta)$ is given by the usual two-loop expression:

$$f(\beta) \simeq \left(\frac{8}{33} \pi^2 \beta \right)^{51/121} \exp \left(-\frac{4}{33} \pi^2 \beta \right), \quad (8)$$

for gauge group $SU(3)$ and in the absence of quarks. At sufficiently large β one also expects that

$$\begin{aligned} \mathcal{D}_\parallel^L f(\beta)^{-4} &= \frac{1}{\Lambda_L^4} \mathcal{D}_\parallel \left(\frac{d^2}{\Lambda_L^2} f^2(\beta) \right), \\ \mathcal{D}_\perp^L f(\beta)^{-4} &= \frac{1}{\Lambda_L^4} \mathcal{D}_\perp \left(\frac{d^2}{\Lambda_L^2} f^2(\beta) \right), \end{aligned} \quad (9)$$

where $f(\beta)$ is given by Eq. (8) and terms of higher order in a are negligible.

In Fig. 2 we plot $\mathcal{D}_\parallel^L f(\beta)^{-4}$ and $\mathcal{D}_\perp^L f(\beta)^{-4}$ versus $d_{\text{phys}} = (d/\Lambda_L) f(\beta)$. In this figure we have also plotted the values of the correlators obtained

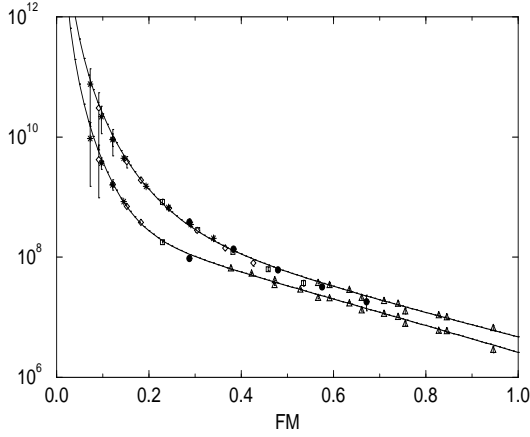


Figure 2. The functions $\mathcal{D}_{\perp}^L f(\beta)^{-4}$ (upper curve) and $\mathcal{D}_{\parallel}^L f(\beta)^{-4}$ (lower curve) versus physical distance (in *fermi* units). Triangles correspond to the data of Ref. [11]. The lines are the curves for \mathcal{D}_{\perp} and \mathcal{D}_{\parallel} obtained from the best fit of Eqs. (10) and (11).

in Ref. [11], corresponding to physical distances $d_{\text{phys}} \geq 0.4$ fm. We have applied a best fit to all of these data with the functions

$$\mathcal{D}_{(1)}(x^2) = A_{(1)} \exp(-|x|/\lambda_A) + \frac{a_{(1)}}{|x|^4} \exp(-|x|/\lambda_a) . \quad (10)$$

We have obtained the following results:

$$\begin{aligned} \frac{A}{\Lambda_L^4} &\simeq 3.3 \times 10^8 , & \frac{A_1}{\Lambda_L^4} &\simeq 0.7 \times 10^8 , \\ a &\simeq 0.69 , & a_1 &\simeq 0.46 , \\ \lambda_A &\simeq \frac{1}{\Lambda_L} \frac{1}{182} , & \lambda_a &\simeq \frac{1}{\Lambda_L} \frac{1}{94} , \end{aligned} \quad (11)$$

with $\chi^2/N_{\text{d.o.f.}} \simeq 1.7$. The continuum lines in Fig. 2 have been obtained using the parameters of this best fit. With the value of Λ_L determined from the string tension [20] we obtain

$$\lambda_A \simeq 0.22 \text{ fm} , \quad \lambda_a \simeq 0.43 \text{ fm} . \quad (12)$$

The correlation length λ_A , which enters the non-perturbative exponential terms of \mathcal{D} and \mathcal{D}_1 , as well as the magnitude of the coefficients A and A_1 , are compatible with the values obtained in Ref. [11].

We stress again that we have been able to observe terms proportional to $1/|x|^4$ in the correlations because we have worked at larger values of β , where the distance between two points (far enough in lattice units so that the correlation is not modified by cooling before lattice artefacts are eliminated) is small compared with 1 fm in physical units. A larger lattice (32^4) has been necessary to avoid infrared artefacts.

3. RESULTS AT FINITE T

To simulate the system at finite temperature, a lattice is used of spatial extent $N_{\sigma} \gg N_{\tau}$, N_{τ} being the temporal extent, with periodic boundary conditions. The temperature T corresponding to a given value of $\beta = 6/g^2$ is given by

$$N_{\tau} \cdot a(\beta) = \frac{1}{T} , \quad (13)$$

where $a(\beta)$ is the lattice spacing, whose expression in terms of β is given by Eqs. (7) and (8).

At finite temperature, the $O(4)$ space-time symmetry is broken down to the spatial $O(3)$ symmetry and in principle the bilocal correlators (1) are now expressed in terms of five independent functions [16–18] (instead of two as in the zero-temperature case); two of them are needed to describe the electric–electric correlations:

$$\langle 0 | \text{Tr} \{ E_i(x) S(x, y) E_k(y) S^\dagger(x, y) \} | 0 \rangle = \delta_{ik} \left[D^E + D_1^E + u_4^2 \frac{\partial D_1^E}{\partial u_4^2} \right] + u_i u_k \frac{\partial D_1^E}{\partial \vec{u}^2} , \quad (14)$$

where $E_i = G_{i4}$ is the electric field operator and $u_\mu = x_\mu - y_\mu$ [$\vec{u}^2 = (\vec{x} - \vec{y})^2$].

Two further functions are needed for the magnetic–magnetic correlations:

$$\langle 0 | \text{Tr} \{ B_i(x) S(x, y) B_k(y) S^\dagger(x, y) \} | 0 \rangle = \delta_{ik} \left[D^B + D_1^B + \vec{u}^2 \frac{\partial D_1^B}{\partial \vec{u}^2} \right] - u_i u_k \frac{\partial D_1^B}{\partial \vec{u}^2} , \quad (15)$$

where $B_k = \frac{1}{2} \varepsilon_{ijk} G_{ij}$ is the magnetic field operator. Finally, one more function, D_1^{BE} , is necessary to describe the mixed electric–magnetic correlations.

The five quantities D^E , D_1^E , D^B , D_1^B and D_1^{BE} are all functions of \vec{u}^2 , due to rotational invariance, and of u_4^2 , due to time-reversal invariance.

From the conclusions of Refs. [16–18], one expects that D^E is related to the (temporal) string tension and should have a drop just above the deconfinement critical temperature T_c . In other words, D^E is expected to be the order parameter of the confinement. Similarly, D^B is related to the spatial string tension [16,17].

We have determined the following four quantities

$$\begin{aligned} \mathcal{D}_{\parallel}^E(\vec{u}^2, 0) &\equiv \mathcal{D}^E(\vec{u}^2, 0) + \mathcal{D}_1^E(\vec{u}^2, 0) + \vec{u}^2 \frac{\partial \mathcal{D}_1^E}{\partial \vec{u}^2} \\ \mathcal{D}_{\perp}^E(\vec{u}^2, 0) &\equiv \mathcal{D}^E(\vec{u}^2, 0) + \mathcal{D}_1^E(\vec{u}^2, 0) \\ \mathcal{D}_{\parallel}^B(\vec{u}^2, 0) &\equiv \mathcal{D}^B(\vec{u}^2, 0) + \mathcal{D}_1^B(\vec{u}^2, 0) + \vec{u}^2 \frac{\partial \mathcal{D}_1^B}{\partial \vec{u}^2} \\ \mathcal{D}_{\perp}^B(\vec{u}^2, 0) &\equiv \mathcal{D}^B(\vec{u}^2, 0) + \mathcal{D}_1^B(\vec{u}^2, 0), \end{aligned} \quad (16)$$

by measuring appropriate linear superpositions of the correlators (14) and (15) at equal times ($u_4 = 0$), on a $16^3 \times 4$ lattice ($N_\tau = 4$, in our notation). The critical temperature T_c for such a lattice corresponds to $\beta_c \simeq 5.69$. The behaviour of $\mathcal{D}_{\parallel}^E$ and \mathcal{D}_{\perp}^E is shown in Figs. 3 and 4 respectively, on three-dimensional plots versus T/T_c and the physical spatial distance. Due to the logarithmic scale, the errors are comparable with the size of the symbols and the lines connecting the points are drawn as an eye-guide. A clear drop is observed for $\mathcal{D}_{\parallel}^E$ and \mathcal{D}_{\perp}^E across the phase transition, as expected.

On the contrary, no drop is visible across the transition for the magnetic correlations $\mathcal{D}_{\parallel}^B$ and \mathcal{D}_{\perp}^B : as an example, the behaviour for \mathcal{D}_{\perp}^B is shown in Fig. 5.

Our results can be summarized as follows:

(i) In the confined phase ($T < T_c$), until very near to the temperature of deconfinement, the correlators, both the electric–electric type (14) and the magnetic–magnetic type (15), are nearly equal to the correlators at zero temperature [14]: in other words, $D^E \simeq D^B \simeq D$ and $\mathcal{D}_1^E \simeq \mathcal{D}_1^B \simeq \mathcal{D}_1$ for $T < T_c$.

(ii) Immediately above T_c , the electric–electric correlators (14) have a clear drop, while the magnetic–magnetic correlators (15) stay almost unchanged, or show a slight increase. More pre-

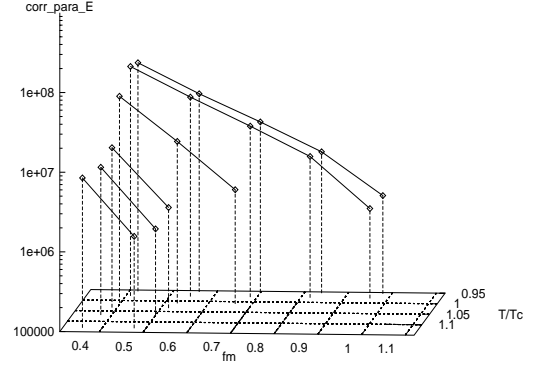


Figure 3. The quantity $\mathcal{D}_{\parallel}^E/\Lambda_L^4$ [defined by the first Eq. (16)] versus T/T_c and the physical spatial distance (in fm).

cisely, looking at the values for the difference

$$\mathcal{D}_{\perp}^E(\vec{u}^2, 0) - \mathcal{D}_{\parallel}^E(\vec{u}^2, 0) = -\vec{u}^2 \frac{\partial \mathcal{D}_1^E}{\partial \vec{u}^2}(\vec{u}^2, 0) \quad (17)$$

between the two quantities reported in Figs. 4 and 3 respectively, one finds that the quantity \mathcal{D}_1^E does not show any drop across the phase transition at T_c . So the clear drop seen in the quantities $\mathcal{D}_{\parallel}^E$ and \mathcal{D}_{\perp}^E across T_c is entirely due to a drop of \mathcal{D}^E alone. This result confirms the conclusion of Refs. [16–18], where \mathcal{D}^E was related to the (temporal) string tension σ_E . Similarly, one can look at the following difference:

$$\mathcal{D}_{\perp}^B(\vec{u}^2, 0) - \mathcal{D}_{\parallel}^B(\vec{u}^2, 0) = -\vec{u}^2 \frac{\partial \mathcal{D}_1^B}{\partial \vec{u}^2}(\vec{u}^2, 0). \quad (18)$$

One thus finds that \mathcal{D}_1^B does not show any drop across the transition and, in addition, it is nearly equal to \mathcal{D}_1^E ($\mathcal{D}_1^B \simeq \mathcal{D}_1^E$). From the fact that the quantities $\mathcal{D}_{\parallel}^B$ and \mathcal{D}_{\perp}^B stay almost unchanged (or even show a slight increase) across T_c , we conclude that the same must be true also for \mathcal{D}^B . It was shown in Refs. [16,17] that \mathcal{D}^B is related to the spatial string tension σ_s . Recent lattice results [21] indicate that σ_s is almost constant around T_c and increases for $T \geq 2T_c$: this fact is in good agreement with the behaviour that we have found for \mathcal{D}^B .

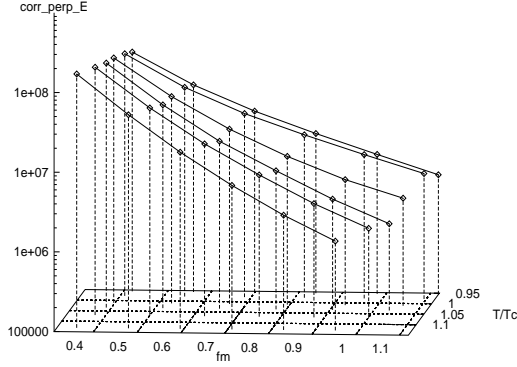


Figure 4. The quantity $\mathcal{D}_{\perp}^E/\Lambda_L^4$ [defined by the second Eq. (16)] versus T/T_c and the physical spatial distance (in fm).

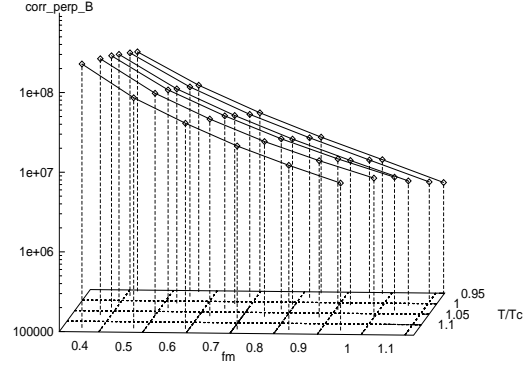


Figure 5. The quantity $\mathcal{D}_{\perp}^B/\Lambda_L^4$ [defined by the fourth Eq. (16)] versus T/T_c and the physical spatial distance (in fm).

ACKNOWLEDGEMENTS

This work was done using the CRAY T3D of the CINECA Inter University Computing Centre (Bologna, Italy). We would like to thank the CINECA for having put the CRAY T3D at our disposal and for the kind and highly qualified technical assistance.

We thank Günther Dosch and Yuri Simonov for many useful discussions.

REFERENCES

1. D. Gromes, Phys. Lett. **115B** (1982) 482.
2. M. Campostrini, A. Di Giacomo and S. Olejnik, Z. Phys. **C31** (1986) 577.
3. Yu.A. Simonov, S. Titard and F.J. Yndurain, Phys. Lett. **B354** (1995) 435.
4. H.G. Dosch, Phys. Lett. **190B** (1987) 177.
5. H.G. Dosch and Yu.A. Simonov, Phys. Lett. **205B** (1988) 339.
6. Yu.A. Simonov, Nucl. Phys. **B324** (1989) 67.
7. O. Nachtmann and A. Reiter, Z. Phys. **C24** (1984) 283.
8. P.V. Landshoff and O. Nachtmann, Z. Phys. **C35** (1987) 405.
9. A. Krämer and H.G. Dosch, Phys. Lett. **252B** (1990) 669.
10. H.G. Dosch, E. Ferreira and A. Krämer, Phys. Rev. D **50** (1994) 1992.
11. A. Di Giacomo and H. Panagopoulos, Phys. Lett. **B285** (1992) 133.
12. M. Campostrini, A. Di Giacomo, M. Maggiore, H. Panagopoulos and E. Vicari, Phys. Lett. **225B** (1989) 403.
13. A. Di Giacomo, M. Maggiore and S. Olejnik, Phys. Lett **236B** (1990) 199; Nucl. Phys. **B347** (1990) 441.
14. A. Di Giacomo, E. Meggiolaro and H. Panagopoulos, Pisa preprint IFUP-TH 12/96 (1996); Cyprus preprint UCY-PHY-96/5 (1996); hep-lat/9603017.
15. A. Di Giacomo, E. Meggiolaro and H. Panagopoulos, Pisa preprint IFUP-TH 14/96 (1996); Cyprus preprint UCY-PHY-96/6 (1996); hep-lat/9603018.
16. Yu.A. Simonov, JETP Lett. **54** (1991) 249.
17. Yu.A. Simonov, JETP Lett. **55** (1992) 627; Yad. Fiz. **58** (1995) 357.
18. Yu.A. Simonov and E.L. Gubankova, Phys. Lett. **B360** (1995) 93.
19. M. Campostrini, A. Di Giacomo and G. Musardo, Z. Phys. **C25** (1984) 173.
20. C. Michael and M. Teper, Nucl. Phys. **B305** (1988) 453.
21. E. Laermann, Nucl. Phys. B (Proc. Suppl.) **42** (1995) 120, and references therein.